

Article

New Approach for Photovoltaic Parameters Extraction for Low-Cost Electronic Devices

Andrés Firman¹, Cesar Prieb², Alexis Raúl González Mayans¹ , Manuel Cáceres¹ , Luis Horacio Vera¹ 
and Juan de la Casa Higuera^{3,*} 

- ¹ Group of Renewable Energies (GER), Northeastern National University, Corrientes 3400, Argentina; afirman@exa.unne.edu.ar (A.F.); raulgonzalezmayans@exa.unne.edu.ar (A.R.G.M.); mcaceres@exa.unne.edu.ar (M.C.); luis.horacio.vera@comunidad.unne.edu.ar (L.H.V.)
- ² LABSOL Laboratório de Energia Solar, Universidade Federal do Rio Grande do Sul, Av. Bento Gonçalves, Porto Alegre 9500, Brazil; cprieb@ufrgs.br
- ³ IDEA Solar Energy Research Group, Electronics and Automation Engineering Department, University of Jaén, Las Lagunillas Campus, 23071 Jaén, Spain
- * Correspondence: delacasa@ujaen.es; Tel.: +34-615-679152

Abstract: This work proposes a new five-parameter model equation for PV devices, which operates as a function of the main representative parameters of PV devices. It is specifically developed for implementation in embedded systems. The methodology presented in this work is notable due to the fact that three of the five parameters can be directly extracted from the experimental current–voltage (I – V) curve, simplifying the iterative process until a pre-set small difference in the determination of the maximum power is achieved. The iterative methodology for extracting the remaining parameters is also described. The proposed methodology is verified by applying it to seven different PV technologies, including crystalline and thin-film technologies. Its parameters are compared with those obtained using the highly precise trust region iterative method. The resulting parameters and the error in the adjustment along the I – V curve are discussed. This methodology demonstrates the capability to accurately adjust the model along the entire I – V curve, determine the maximum power, and is not dependent on highly variable parameters.



Citation: Firman, A.; Prieb, C.; González Mayans, A.R.; Cáceres, M.; Vera, L.H.; de la Casa Higuera, J. New Approach for Photovoltaic Parameters Extraction for Low-Cost Electronic Devices. *Energies* **2023**, *16*, 4956. <https://doi.org/10.3390/en16134956>

Academic Editor: Michel Piliouguine Rocha

Received: 16 March 2023

Revised: 16 June 2023

Accepted: 20 June 2023

Published: 26 June 2023



Copyright: © 2023 by the authors. Licensee MDPI, Basel, Switzerland. This article is an open access article distributed under the terms and conditions of the Creative Commons Attribution (CC BY) license (<https://creativecommons.org/licenses/by/4.0/>).

Keywords: photovoltaics; electrical characterization; five-parameter electrical model; I – V curve

1. Introduction

In recent years, there has been a significant global interest in photovoltaic (PV) technology [1,2]. This interest has been encouraged by the potential for improved reliability and decreasing costs. Ongoing research is focused on continuously increasing the efficiency of PV technology, with some studies reporting efficiencies above 22% [3,4]. Furthermore, the outdoor lifetime of PV modules has been observed to extend beyond 20 years [5,6].

Concurrently, various electronic devices, such as current–voltage (I – V) curve tracers, have been designed. However, low-cost electronic devices are unable to perform the necessary parameter extraction required to obtain the electrical equivalent model of photovoltaic modules, or they are very unusual. This is due to the absence of I – V curve tracers in the market that allow us to obtain the main characteristic parameters of the electrical equivalent model. This limitation is due to the high computational load associated with such extractions. The electrical characterization of PV modules is essential as it allows for finding the electrical equivalent circuit, which can be used for modeling purposes. For example, this modeling can facilitate the study of long-term power degradation [7–10] and aid in translation to standard test conditions (STC). Therefore, parameter extraction is crucial for predicting or modeling the performance of PV devices under different environmental conditions and asserting their power output.

The objective of this work is to propose a parameter extraction method that can be implemented in devices with low computational resources, such as low-cost embedded

systems, without compromising the accuracy of the process. Ultimately, the goal is to obtain an equivalent electrical model to allow translation of the results to STC within these devices while correctly determining the maximum power point.

It should be noted that the authors of this study have prior experience in the design and development of low-cost I - V tracers for educational purposes [11,12] and that the proposed designs are working successfully in multiple research laboratories. As an extension of this previous work, the intention is to improve the functionality of the system by adding in-circuit parameter extraction and translation capabilities.

The existing literature offers several models and methods for performing parameter extraction. These include three, four, and five single-diode parameter models, where each element represents a different electrical behavior in the PV cell. Some models even attempt to enhance their features by incorporating two or even three diodes, resulting in the three-diode seven-parameter model [13–16]. Each method is supposed to increase precision but at the expense of increased computational load. Furthermore, in some cases, it becomes challenging to interpret each of these parameters from a practical or physical perspective due to their variability.

Regardless of the chosen model, determining the parameters for the equivalent circuit model of PV devices under test involves different approaches in the literature. Some authors [17–19] utilize iterative methods to perform a numerical adjustment on the experimental I - V curve. On the other hand, others propose simpler calculation equations based on key representative points of the I - V curve [20] but do not always assert the maximum power point (P_M).

In this study, a new single-diode five-parameter model equation is proposed. This equation is based on the main representative values directly extracted from the I - V curve, aiming to simplify the process while working with parameters that exhibit high repeatability. Additionally, an associated iterative methodology is presented, with the primary goal of reliably estimating the P_M . This estimation is crucial for accurately assessing PV module performance. The iterative method introduced in this work employs variables that can be linked to physical parameters, ensuring that it goes beyond a mere mathematical fitting of the experimental I - V curve data. Therefore, facilitating its convergence and, consequently, reducing the processing time.

The five-parameter single-diode model is considered the most versatile model among those presented in the literature [8,13,21,22]. Consequently, it was selected as the model of choice for this study. However, one of the main challenges associated with this model is that its equation is in implicit form, making it difficult to determine its parameters [8,22,23].

The primary advantage of the five-parameter model is its simplicity and suitable representation of the entire I - V curve. Moreover, it does not require excessive computational load compared to more complex models, and it can be easily explained from both electrical and physical perspectives. These factors make it the fundamental model employed in this research.

This paper will compare the results of a proposed methodology for parameter extraction from a set of I - V curves with the so-called “trust region” method [24], which involves a high computational load. That methodology relies on a significant number of adjusted curves to identify the best fit. It is a technique commonly employed for solving optimization problems, including parameter estimation in mathematical models [25,26].

The trust region method operates by iteratively adjusting the parameters of the model within a specified region or “trust region” based on suitable data. It aims to find the optimal set of parameters that best fit the data while adhering to a certain variability range. During each iteration, the method evaluates the objective function (in this case, the discrepancy between the model predictions and the observed data) within the trust region. Based on this evaluation, it determines whether to accept or reject the current set of parameters and adjusts the trust region according to its root mean square (RMS) error.

Equivalent Circuit of Five-Parameter Single-Diode Model

Figure 1 illustrates the equivalent electrical circuit model of the five-parameter single-diode model.

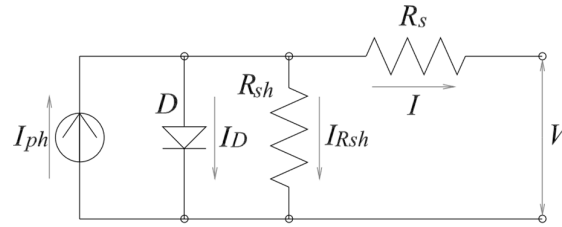


Figure 1. Equivalent electrical circuit model of the five-parameter single-diode model.

In this model, I_{ph} represents the photogenerated current, which indicates the current generated by the illuminated photovoltaic device. It is essentially the current source that delivers electrical energy through the photovoltaic effect [21,27].

Diode D represents the PN junction necessary to establish an electric field that enables the movement of electrons out of the photovoltaic cell. I_D represents the current flowing through diode D .

R_{sh} corresponds to the shunt resistance, which acts as a parasitic resistance through which the current I_{Rsh} flows. It represents a portion of current deviated from the photogenerated current and can be understood as a conduction path within the PV cell. The presence of R_{sh} leads to a decrease in overall efficiency.

Finally, R_s denotes the series resistance through which the output current I flows. It is another parasitic resistance that induces a voltage drop due to internal resistance and interconnection between cells. The voltage established at the output terminals of the device is V .

From the equivalent electrical circuit, we can express the output current as $I = I_{ph} - I_D - I_{Rsh}$. By substituting I_D with the diode equation, which is expressed by Shockley (1949) [28,29], and I_{Rsh} with Ohm's law, we obtain Equation (1).

$$I = I_{ph} - I_0 \left[\exp\left(\frac{V + I R_s}{m N_s V_t}\right) - 1 \right] - \frac{V + I R_s}{R_{sh}}. \quad (1)$$

In Equation (1), the following parameters are defined:

I : Output current corresponding to the voltage V .

I_{ph} : Photogenerated current.

I_0 : Diode reverse saturation current.

m : Diode ideality factor.

N_s : Number of series connected cells.

V_t : Thermal voltage ($V_t = kT/q$, where k is the Boltzmann constant, T is the absolute temperature, and q is the electron charge).

R_{sh} : Shunt resistance.

R_s : Series resistance.

Equation (1) is an implicit equation for I , and it remains valid for cells, modules, and PV generators by considering an appropriate value for N_s [30].

Various authors have focused their efforts on minimizing the number of parameters that need to be determined. This simplifies the iterative adjustment process and reduces the computational load required [31]. However, other authors prioritize achieving a mathematically precise adjustment along the entire I - V characteristic curve, which may interpret the results as challenging or impractical [32].

The present study builds upon the equivalent circuit of the five-parameter single-diode model, where some parameters can be easily determined from the I - V curve. It introduces a detailed new methodology that incorporates an iterative adjustment process to accurately

estimate the electric behavior of PV devices and their maximum power point (P_M). The study also includes an analysis of the reliability of the estimated results.

The developed methodology is based on a modified form of Equation (1) to reduce the number of parameters that need to be determined. Out of the five parameters, three can be easily extracted through simple observations of the I - V curve. The remaining two parameters are determined based on their physical behavior until a suitable difference around the (P_M) is achieved because this is considered the most significant on the I - V curve.

By employing this approach, the study aims to streamline the parameter determination process. Furthermore, it emphasizes the importance of accurately estimating the behavior around the maximum power point, which is crucial for the overall performance analysis of PV systems as degradation processes over time.

The methodology is validated by employing experimental characterization of I - V curves under simulated sunlight. Since one of the objectives of this paper is to validate the precision of the proposed method, it is important to limit the uncertainties that a characterization in the real sun could shed on the results. Additionally, we compare them with the precise iterative method known as the “trust region” method.

2. New Five-Parameter Model Equation and Iterative Adjusting Methodology

From the perspective of the equivalent circuit, the electric characterization of a PV device requires an experimental I - V curve. This curve can be mathematically adjusted according to the chosen electrical model to determine the values of its electrical parameters.

In this case, it is convenient, in terms of repeatability, to avoid using the I_0 and I_{ph} currents in the fundamental equation. This current is challenging to determine experimentally and often exhibits significant inconsistency between tests. Instead, the equation can be rearranged using other parameters that can be easily obtained from the I - V curve.

In order to illustrate this, let us consider the short-circuit condition and refer to Figure 1. In this case, we can assert that I flows on R_s and V is equal to 0, and the resistances are connected in parallel. If the voltage across R_s in parallel with R_{sh} is not significant enough to forward bias the diode D , the current I_D tends to be practically zero. Hence, writing I as $I_{SC} = I_{ph} - I_{R_{sh}}$. Applying Ohm’s law, we obtain Equation (2).

$$I_{ph} = I_{SC} \left(1 + \frac{R_s}{R_{sh}} \right). \quad (2)$$

Equation (2) provides a relationship between I_{ph} and I_{SC} , taking into account the losses caused by resistances R_s and R_{sh} .

Similarly, if we consider the open-circuit condition where V is equal to V_{OC} and I is equal to 0, we can rewrite Equation (1) as Equation (3).

$$0 = I_{ph} - I_0 \left[\exp \left(\frac{V_{OC}}{m N_s V_t} \right) - 1 \right] - \frac{V_{OC}}{R_{sh}}. \quad (3)$$

In the case of a properly functioning PV module, the exponential term in Equation (3) is typically much larger than 1, often approximately on the order of magnitude of $\exp(20)$. Therefore, we can approximate Equation (3) and obtain Equation (4).

$$I_0 = \left(I_{ph} - \frac{V_{OC}}{R_{sh}} \right) \left[\exp \left(-\frac{V_{OC}}{m N_s V_t} \right) \right]. \quad (4)$$

By substituting the expression for I_{ph} from Equation (2) into Equation (4), we obtain Equation (5). In this equation, current I_0 can be easily determined by knowing I_{SC} , the losses resistances (R_s and R_{sh}), and V_{OC} .

$$I_0 = \left[\frac{I_{SC}(R_s + R_{sh}) - V_{OC}}{R_{sh}} \right] \left[\exp \left(-\frac{V_{OC}}{m N_s V_t} \right) \right]. \quad (5)$$

Therefore, by utilizing Equations (2) and (5), we can eliminate the inconvenience of directly determining the I_0 current, which can be challenging in practice. Substituting these expressions into Equation (1), performing the necessary operations, and neglecting the contribution of a small negative exponential term (which is approximately $1/\exp(20)$ in magnitude and significantly smaller than 1), we obtain a new equation, Equation (6), that is independent of I_0 and I_{ph} .

$$I = I_{SC} \left(\frac{R_s + R_{sh}}{R_{sh}} \right) - \frac{I_{SC}(R_s + R_{sh}) - V_{OC}}{R_{sh}} \left[\exp \left(\frac{V - V_{OC} + I R_s}{m N_s V_t} \right) \right] - \frac{V + I R_s}{R_{sh}}. \tag{6}$$

Equation (6) is more convenient for performing iterative parameter adjusting over the I - V curve, especially under normal operating conditions, as it is a function of the main macro parameters. Among the five parameters, I_{SC} and V_{OC} can be easily determined. This reduces the problem of finding the remaining three parameters: m , R_s , and R_{sh} , as we will explain in the following sections, which is also an advantage for characterization and modeling purposes.

For the determination of R_{sh} , we evaluate the slope in the proximity of I_{SC} . By considering Equation (1) in the vicinity of the short-circuit condition, we can neglect the contribution of diode conduction. This allows us to write I as $I_{ph} - (V + I R_s)/R_{sh}$. Taking the derivative of this expression with respect to V , we obtain Equation (7).

$$\frac{\partial I}{\partial V} = - \frac{1}{(R_{sh} - R_s)}. \tag{7}$$

For a properly operating PV device, it is typically observed that $R_s \ll R_{sh}$ (on the order of magnitude of 100). In this case, we can approximate the inverse of R_s with its sign changed to determine R_{sh} in the vicinity of the short-circuit current I_{SC} . Therefore, R_{sh} can be directly calculated from the data obtained from the experimental I - V curve, as shown in Equation (8).

$$- \frac{1}{\frac{\partial I}{\partial V}} \Big|_{I_{SC}} \approx R_{sh}. \tag{8}$$

On the other hand, it is important to note that the proximity of V_{OC} is similar to the aforementioned case. However, in this scenario, we neglect the contribution of $I_{R_{sh}}$ in comparison to I_{R_s} , because it can be demonstrated that R_{sh} has a low influence in the V_{OC} region. Therefore, we can express I as $I_{ph} - I_D$. Taking the derivative of this expression with respect to V , we obtain Equation (9).

$$\frac{\partial I}{\partial V} = -I_0 \left(\frac{1 + \frac{\partial I}{\partial V} R_s}{m N_s V_t} \right) \left[\exp \left(\frac{V + I R_s}{m N_s V_t} \right) \right]. \tag{9}$$

Next, by solving the equation for $\partial I/\partial V$ in Equation (9), taking its inverse, and changing its sign, we obtain Equation (10). This equation reveals that in the vicinity of V_{OC} , the slope is determined by two unknown parameters, m and R_s (I_0 may be determined using Equation (2)). Increasing both parameters will result in a decrease in the slope towards the same side.

$$- \frac{1}{\frac{\partial I}{\partial V}} \Big|_{V_{OC}} = \frac{m N_s V_t}{I_0 \exp \left(\frac{V_{OC}}{m N_s V_t} \right)} + R_s. \tag{10}$$

Observing Equation (10), we can conclude that the slope is influenced by three unknown parameters: m , I_0 , and R_s . However, solving this equation algebraically can be challenging. Both terms in the equation have the same sign and affect the slope similarly. As a result, we can employ an iterative method where that slope serves as an initial value for R_s . Then, we gradually decrease R_s in small steps until we achieve a predefined small difference for P_M .

Additionally, we can estimate the value of R_s by starting with an initial value for m . In the literature, a common initial value for m is taken as 1, representing the ideal case (minimum value) [28,29]. By setting an upper limit for R_s , we can assess the difference in the maximum power point compared to the experimental case.

Here is the algorithmic workflow for this approach:

1. Calculate the slope with its sign changed in the vicinity of V_{OC} , and designate this as the initial R_s value or seed. It should be set as a maximum value. We start with $m = 1$, which represents a minimum value.
2. Using Equation (6), increment m and decrement R_s in small steps until a small pre-set difference for P_M is achieved.

If the computational load is not a concern, for each decrement of R_s , we can calculate an entire range of m to find the best fit. However, if the computational load is an issue, how we perform the increment and decrement will directly impact the result. Nonetheless, the computational load can be adjusted by selecting suitable steps for each value, adjusting the length of the data array to be calculated, and choosing a predefined difference for P_M .

Therefore, using Equation (6), we have an implicit equation that depends on I_{SC} , V_{OC} , R_{sh} , m , and R_s . The last three parameters can be determined by applying Equation (8) to obtain R_{sh} , followed by an iterative process to obtain the values of m and R_s .

Finally, if the determination of I_{ph} and I_0 is required, we can utilize Equation (2) for I_{ph} and Equation (5) for I_0 , respectively.

3. Experimental Validation of the Proposed Method

In order to test the proposed methodology, seven PV modules of different technologies were evaluated. The evaluated technologies included monocrystalline (mC), polycrystalline (pC), Copper–Indium–Selenide (CIS), Copper–Indium–Gallium–Selenide (CIGS), Cadmium–Telluride (CdTe), amorphous silicon (a-Si), and heterojunction with an intrinsic thin layer (HIT).

The I – V curves were obtained using an A-class solar simulator, as shown in Figure 2, with controlled temperature chamber (1000 W/m^2 and cell temperature of $25 \text{ }^\circ\text{C}$), ensuring these states and keeping them constant. The solar simulator is equipped with an electronic charge and data acquisition system. The data acquisition process resulted in a dataset of approximately 250 valid data points for the entire I – V curve [33].

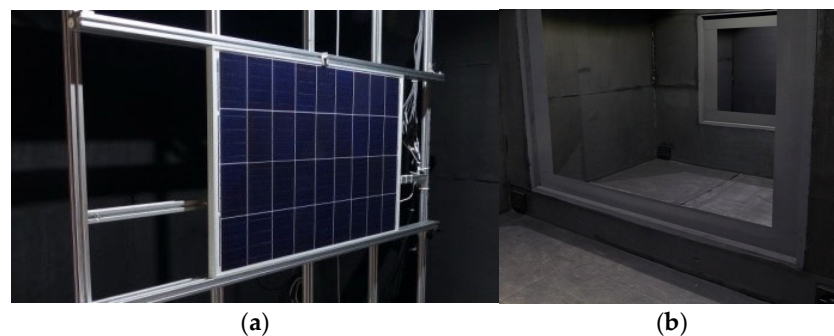


Figure 2. Photographs of the solar simulator. (a) Module mount; (b) Light source–collimator set.

The PV module was exposed to collimated sunlight during the flash, which had a duration of 10 ms. The module was installed on a perpendicular plane, which had a useful area of $2 \text{ m} \times 2 \text{ m}$. The electronic load was activated during the 10 ms to trace the I – V curve, and this process was controlled by a computer.

To compare the results and analyze their behaviors, a set of I – V curves from different PV module technologies was used. The goal was to determine if the results obtained for each methodology were suitable in each case.

To evaluate the percentage difference or percentage error (*Error* %) between the adjusted and experimental curves, Equation (11) was utilized. In this equation, P_i represents the experimental power data, and P'_i represents the adjusted power data. The error was

then evaluated across the entire curve relative to its maximum power (P_M). The inclusion of P_M in the expression helped to avoid indetermination in the cases where $P = 0$.

$$\text{Error \%} = \left(\frac{P_i - P'_i}{P_M} \right) 100. \quad (11)$$

4. Comparative Results from the Experimental I - V Curves

The parameters obtained from the five-parameter single-diode model are presented in Table 1. These parameters were calculated using the proposed adjusting (A) methodology, and for comparison, the values calculated by the trust region (TR) methodology are also provided.

Table 1. Results obtained from the adjusted methodology presented (A), together with the trust region method (TR). Between the square brackets, the RMS error and the maximum experimental power are indicated.

Module (Ref) and [RMS Error]	R_{sh} (Ω)	R_s (Ω)	m	I_0 (A)	I_{ph} (A)	P_M (W) and [exp. P_M]
mC (TR) [0.0414]	9970	0.17	1.18	1.85×10^{-9}	11.51	446.3 [451.3]
mC (A)	253	0.18	1.01	3.63×10^{-11}	11.57	451.0
pC (TR) [0.0656]	$>1 \times 10^4$	0.21	1.37	8.92×10^{-8}	11.33	403.9 [408.7]
pC (A)	247	0.26	1.11	9.23×10^{-10}	11.37	408.7
CIS (TR) [0.0085]	487	2.7	1.86	1.73×10^{-5}	3.36	115.5 [115.8]
CIS (A)	493	2.7	1.81	1.12×10^{-5}	3.35	115.8
CIGS (TR) [0.0090]	292	1.9	2.05	5.27×10^{-6}	2.60	136.0 [136.3]
CIGS (A)	429	1.5	2.35	2.42×10^{-5}	2.58	136.3
CdTe (TR) [0.0023]	1002	1.2	2.71	4.23×10^{-4}	1.77	91.7 [91.6]
CdTe (A)	976	1.4	2.64	3.26×10^{-4}	1.76	91.6
a-Si (TR) [0.0101]	406	0.6	1.52	4.37×10^{-7}	3.38	149.9 [150.2]
a-Si (A)	713	0.5	1.64	1.35×10^{-6}	3.37	150.2
HIT (TR) [0.0209]	$>1 \times 10^{10}$	0.5	1.70	1.10×10^{-5}	6.00	294.2 [297.4]
HIT (A)	2157	0.6	1.52	2.35×10^{-6}	6.01	297.4

The table includes the seven module technologies used in this study. The calculated values for I_0 and I_{ph} are also presented, providing the complete set of parameters for the classical five-parameter model.

From the traced I - V curves, I_{SC} and V_{OC} were easily extracted by reading directly from the curves. As mentioned earlier, the inverse slope method was employed to determine R_{sh} by the slope in the proximity of the short-circuit current. A maximum value of R_s was obtained with the slope in the proximity of the open-circuit voltage by starting with an m seed value of 1. Using an iterative process, m was incrementally adjusted in small steps, and R_s was recalculated until a minimal difference for the maximum power point was achieved (pre-set to $\pm 0.1\%$).

When comparing the parameter values obtained through the methodologies, it was observed that there was high variability in the R_{sh} values, even varying by more than one order of magnitude. This variation may be attributed to the different approaches used by the methodologies to extract R_{sh} . Even more, this discrepancy can be attributed to the effect of electrical noise during the curve tracing, where even small changes can result in significant alterations in the slope, particularly in this nearly horizontal slope.

However, for R_s and m , the proposed methodology tended to yield similar values. In the case of I_0 , significant differences were observed, varying by one or two orders of magnitude. This is in accordance with the literature, which often reports substantial differences in this parameter, even among different I - V curves of the same PV module. Hence, the present methodology avoided utilizing I_0 . This discrepancy can be attributed

to the fact that I_0 is a very small value and has a significant influence on the curvature or “knee” region of the I – V curve.

Nevertheless, in all cases, the adjusted methodology ensures that a difference smaller than 0.1% of P_M is achieved with the proposed method, surpassing the performance of the trust region methodology. Although the TR methodology consistently presents a low root mean square (RMS) error across the entire curve, it is not specifically focused on the maximum power point. Even so, the proposed methodology is able to achieve the main goal of precisely adjusting the maximum power of the PV device, enabling repeatability in future studies stemming from this work.

Regarding I_{ph} , the fitting methodology yields almost the same values consistently.

Thus from Equation (6), we can extract or model an I – V curve as a function of R_s , R_{sh} , V_{OC} , I_{SC} , and m , instead of R_s , R_{sh} , I_{ph} , I_0 , and m .

4.1. Result from Adjusted Parameters and Experimental I – V Curves

To illustrate the methodology, Figure 3 displays the experimental I – V curves that were traced, with one curve for each tested module. These curves are graphically presented in shared plots. The experimental dataset is represented using “bubble plots”, while the fitted curves are represented by continuous lines. The resulting error curve is shown with its values on the right axis, indicated by a scale labeled as Error (%). A horizontal reference line at zero percent is included for reference, along with a vertical trace line indicating the voltage corresponding to the maximum power point (V_M).

4.1.1. mC PV Module

Examining Figure 3a, for the first crystalline technology, the monocrystalline PV module, we can observe that the error % curve exhibits significant variations around the P_M point, both in excess and in defect, reaching differences of up to -3% in that region. Several factors could explain this, such as electrical noise observed in the “knee” region, a change in the slope towards V_{OC} , the inability of the adjusted methodology to accurately determine the m value (which has a major influence in this region), or even abrupt changes in the curve (mismatch). However, regardless of these fluctuations, the P_M point is consistently located with precision within $\pm 0.1\%$, as intended in this study. The remainder of the curve demonstrates high precision in the adjustment over the plain zone towards I_{SC} .

4.1.2. pC PV Module

In the case of the polycrystalline PV module, Figure 3b, we can observe a behavior similar to the mC module around the P_M point, with variations in excess and defect on both sides. Additionally, there is noticeable electrical noise present in the “knee” region, which can potentially affect the accuracy of the adjustment in that area. As a result, the error % fluctuates between $\pm 2\%$. However, despite these fluctuations, P_M point is still determined with precision in the same range.

4.1.3. CIS PV Module

The curves obtained from the first thin-film module tested are depicted in Figure 3c. The CIS curve demonstrates excellent performance in its adjustment with the experimental data. However, the error curve exhibits electrical noise throughout the entire I – V curve, likely due to the electronic load or fluctuations on the light source, reaching an amplitude of approximately $\pm 0.1\%$.

Despite this noise, the maximum error observed is around 0.6%. The higher R_s value can be attributed to a larger number of cell series interconnected, which is commonly associated with thin-film technologies [34–37]. The m parameter deviates from the ideal case as it tends to “round out” the knee of the curve. This deviation could be attributed to an increase in dissimilar crystal ordering within the cell, which is often associated with the fabrication process [38,39].

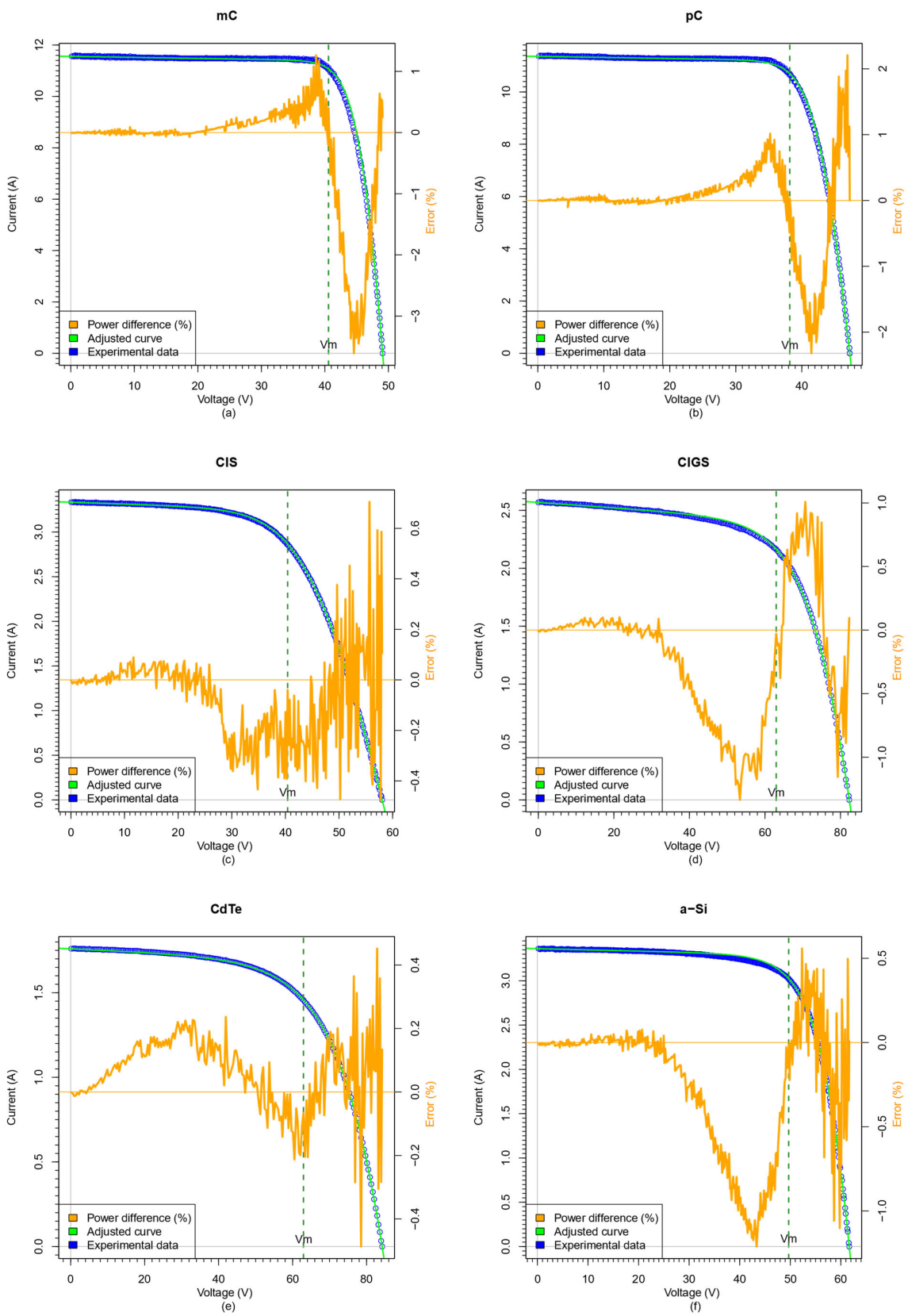


Figure 3. Cont.

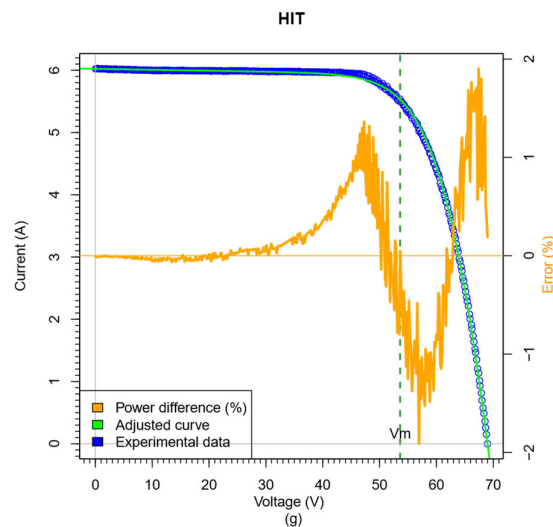


Figure 3. I - V plots; experimental I - V curves, I - V adjusted curves, and error curves for the seven PV technologies tested. For (a) monocrystalline (mC), (b) polycrystalline (pC), (c) Copper–Indium–Selenide (CIS), (d) Copper–Indium–Gallium–Selenide (CIGS), (e) Cadmium–Telluride (CdTe), (f) amorphous silicon (a-Si), (g) and heterojunction with an intrinsic thin layer (HIT).

4.1.4. CIGS PV Module

In the case of the CIGS module tested, its curves are depicted in Figure 3d. The adjusted curve exhibits slight differences in the region surrounding the P_M point. These differences are evident in the error curve, indicating both excess and defect around the P_M , with maximum values reaching approximately 1.3%. However, the power is successfully fitted within a tolerance of 0.1%. Additionally, there is a noticeable difference in curvature on both sides between the experimental and adjusted curves.

This effect could be attributed to a slight electrical mismatch between each half of the PV module or a lack of precision in the five-parameter model used to represent it.

4.1.5. CdTe PV Module

Figure 3e displays the CdTe module, as mentioned earlier. The fitting achieves an accuracy of under $\pm 0.5\%$ for the majority of the curve, indicating excellent performance in the adjustment process. However, there is still some presence of electrical noise, particularly noticeable in the V_{OC} region. Nevertheless, we can confidently state that the adjustment was successfully applied along the entire I - V curve and accurately located the P_M point.

4.1.6. a-Si PV Module

On the other hand, Figure 3f illustrates the curves of the a-Si PV module. Similarly, these curves exhibit an unclear fit with variations in excess and defect around the P_M point, resulting in an error beyond $\pm 1.0\%$ for the overall dataset. However, the approximation improves significantly to below 0.1% for the P_M point.

This difference primarily occurs on the left side of V_M , possibly due to an electrical mismatch effect present in the PV module, which induces a slight drop. Consequently, the error curve displays a small region near the P_M point where the error reaches approximately -1.0% .

4.1.7. HIT PV Module

Figure 3g illustrates the curves obtained for the HIT PV module. Similar to the crystalline module, we can observe significant discrepancies and noise around the P_M point, with errors reaching approximately $\pm 2\%$. However, it is important to note that despite the dispersion caused by the noise generated by the tracer load, the P_M point is

accurately determined within the set range. Nonetheless, due to the noise present, the reliability of the results is affected.

4.2. Results and Facts

Analyzing the results obtained by applying the proposed methodology, we can make the following assertions: The methodology can extract a suitable model to represent the performance characteristics of PV devices across various technologies, except for the proper determination of R_{sh} .

It avoids the determination of highly variable parameters, such as I_0 , by utilizing I_{SC} and m instead.

5. Conclusions

This paper presents a new model equation for the five-parameter equivalent circuit as a function of the main macro values that can be easily extracted from an experimental I - V curve, such as I_{SC} , V_{OC} , R_{sh} , m , and R_s . Additionally, an iterative methodology to obtain values for m and R_s is explained in detail, tested, and compared to a method considered as a standard reference.

In the proposed mathematical model, very small approximations and neglects were made, which helps simplify the fitting process. As a result, three of the five model parameters can be determined almost directly from a straightforward analysis of the experimental I - V curve. Therefore, the problem is reduced to adjusting only two related parameters: m and R_s . The procedure to obtain seed values for m and R_s is also shown. Consequently, the equation becomes a function of the main macro parameters of the I - V curve, such as I_{SC} and V_{OC} , instead of other parameters that are more difficult to obtain directly, such as I_0 and I_{ph} . Furthermore, the conversion equations between these parameters are presented.

The main advantage of this approach is to avoid highly dispersive parameters that can affect comparative studies, for example, studies related to the degradation process. This new equation leads to a more suitable method for extracting the main electrical parameters that describe the operation of PV devices based on the main I - V parameters. This is particularly significant when considering the implementation of these algorithms on low-cost hardware devices with limited computational capacity.

The five electrical parameters were applied to seven different PV module technologies. Based on the observation of the percentage difference of errors obtained for the entire data set, it indicates a high disparity in some cases. These errors primarily occur near the proximity of the maximum power point and the V_{OC} . They are interpreted as slight differences between the module's actual behavior and the behavior assumed by the equivalent model. This difference is mainly attributed to the diode model, as its influence zone (m) or "knee" zone exhibits different curvatures on both sides of the maximum power point, and due to noise present in the I - V curve tracer or in the light source.

For all cases, the deviation between the experimental and adjusted data was below 0.1% of P_M , demonstrating reliability in its determination, achieving one of the main goals, and resulting in the main advantage of the method, compared with others.

The simplicity of this new method allows for its incorporation into embedded hardware, enabling operation without the need for a personal computer. Only the extraction of V_{OC} , I_{SC} , and the slopes in these regions of the I - V curve is required, tasks easily achievable for small, low-cost devices. An iterative process that varies the seed values (R_s and m) in opposite directions leads to the determination of the remaining parameters.

This paper can be further expanded or extended as a translation methodology by incorporating models for the variation of V_{OC} and I_{SC} with temperature and irradiance. Such models would be useful for testing modules under any kind of light, e.g., natural sunlight or simulated sunlight. Additionally, Equation (6) presented in this paper may be more convenient for simulation purposes on various computational platforms. It is easy to interpret, modify, and adapt to different operating conditions, providing flexibility, versatility, and usability in different scenarios.

Finally, the presented methodology effectively represents the behavior of PV modules and may be easily adaptable to embedded electronics systems.

Author Contributions: Conceptualization, A.F., M.C. and J.d.I.C.H.; Methodology, C.P. and A.R.G.M.; Software, C.P., A.R.G.M. and M.C.; Validation, C.P., M.C., L.H.V. and J.d.I.C.H.; Formal analysis, Cesar Prieb, L.H.V. and J.d.I.C.H.; Investigation, A.F.; Writing—original draft, A.F.; Supervision, M.C.; Funding acquisition, L.H.V. All authors have read and agreed to the published version of the manuscript.

Funding: This research received no external funding.

Data Availability Statement: Not applicable.

Conflicts of Interest: The authors declare no conflict of interest.

References

1. Munshi, A.H.; Sasidharan, N.; Pinkayan, S.; Barth, K.L.; Sampath, W.S.; Ongsakul, W. Thin-film CdTe photovoltaics—The technology for utility-scale sustainable energy generation. *Sol. Energy* **2018**, *173*, 511–516. [[CrossRef](#)]
2. Elanzeery, H.; Babbe, F.; Melchiorre, M.; Werner, F.; Siebentritt, S. High-performance low bandgap thin film solar cells for tandem applications. *Prog. Photovolt.* **2018**, *26*, 437–442. [[CrossRef](#)]
3. Kato, T.; Wu, J.L.; Hirai, Y.; Sugimoto, H.; Bermudez, V. Record efficiency for thin-film polycrystalline solar cells up to 22.9% achieved by Cs-treated Cu (In, Ga)(Se, S) 2. *IEEE J. Photovolt.* **2018**, *9*, 325–330. [[CrossRef](#)]
4. Kamada, R.; Yagioka, T.; Adachi, S.; Handa, A.; Tai, K.F.; Kato, T.; Sugimoto, H. New world record Cu (In, Ga)(Se, S) 2 thin film solar cell efficiency beyond 22%. In Proceedings of the 2016 IEEE 43rd Photovoltaic Specialists Conference (PVSC), Portland, OR, USA, 5–10 June 2016; pp. 1287–1291. [[CrossRef](#)]
5. Aghaei, M.; Fairbrother, A.; Gok, A.; Ahmad, S.; Kazim, S.; Lobato, K.; Kettle, J. Review of degradation and failure phenomena in photovoltaic modules. *Renew. Sust. Energ. Rev.* **2022**, *159*, 112160. [[CrossRef](#)]
6. Ameer, A.; Berrada, A.; Bouaichi, A.; Loudiyi, K. Long-term performance and degradation analysis of different PV modules under temperate climate. *Renew. Energ.* **2022**, *188*, 37–51. [[CrossRef](#)]
7. Gnetchejo, P.J.; Essiane, S.N.; Ele, P.; Wamkeue, R.; Wapet, D.M.; Ngoffe, S.P. Important notes on parameter estimation of solar photovoltaic cell. *Energy Convers. Manag.* **2019**, *197*, 111870. [[CrossRef](#)]
8. Ayang, A.; Wamkeue, R.; Ouhrouche, M.; Malwe, B.H. Maximum Likelihood Parameters Estimation of Single-Diode Photovoltaic Module/Array: A Comparative Study At STC. In Proceedings of the 2018 IEEE Electrical Power and Energy Conference (EPEC), Toronto, ON, Canada, 10–11 October 2018; pp. 1–6. [[CrossRef](#)]
9. Lidaighbi, S.; Elyaqouti, M.; Assalaou, K.; Hmamou, D.B.; Saadaoui, D.; H'roua, J. Parameter estimation of photovoltaic modules using analytical and numerical/iterative approaches: A comparative study. *Mater. Today* **2022**, *52*, 1–6. [[CrossRef](#)]
10. Yilmaz, P.; Schmitz, J.; Theelen, M. Potential induced degradation of CIGS PV systems: A literature review. *Renew. Sust. Energ. Rev.* **2022**, *154*, 111819. [[CrossRef](#)]
11. Cáceres, M.; Firman, A.; Montes-Romero, J.; González Mayans, A.R.; Vera, L.H.; Fernández, E.; de la Casa Higuera, J. Low-cost I–V tracer for PV modules under real operating conditions. *Energies* **2020**, *13*, 4320. [[CrossRef](#)]
12. Montes-Romero, J.; Torres-Ramírez, M.; De la Casa, J.; Firman, A.; Cáceres, M. Software tool for the extrapolation to Standard Test Conditions (STC) from experimental curves of photovoltaic modules. In Proceedings of the 2016 Technologies Applied to Electronics Teaching (TAEE), Seville, Spain, 22–24 June 2016; pp. 1–7. [[CrossRef](#)]
13. Drouiche, I.; Harrouni, S.; Arab, A.H. A new approach for modelling the aging PV module upon experimental I–V curves by combining translation method and five-parameters model. *Electr. Power Syst. Res.* **2018**, *163*, 231–241. [[CrossRef](#)]
14. Qais, M.H.; Hasanien, H.M.; Alghuwainem, S. Parameters extraction of three-diode photovoltaic model using computation and Harris Hawks optimization. *Energy* **2020**, *195*, 117040. [[CrossRef](#)]
15. Pardhu, B.G.; Kota, V.R. Radial movement optimization based parameter extraction of double diode model of solar photovoltaic cell. *Sol. Energy* **2021**, *213*, 312–327. [[CrossRef](#)]
16. Rasheed, M.; Shihab, S.; Mohammed, O.Y.; Al-Adili, A. Parameters Estimation of Photovoltaic Model Using Nonlinear Algorithms. *J. Phys. Conf. Ser.* **2021**, *1795*, 012058. [[CrossRef](#)]
17. Soliman, M.A.; Al-Durra, A.; Hasanien, H.M. Electrical parameters identification of three-diode photovoltaic model based on equilibrium optimizer algorithm. *IEEE Access* **2021**, *9*, 41891–41901. [[CrossRef](#)]
18. Chen, Z.; Chen, Y.; Wu, L.; Cheng, S.; Lin, P.; You, L. Accurate modeling of photovoltaic modules using a 1-D deep residual network based on IV characteristics. *Energy Convers. Manag.* **2019**, *186*, 168–187. [[CrossRef](#)]
19. Wu, L.; Chen, Z.; Long, C.; Cheng, S.; Lin, P.; Chen, Y.; Chen, H. Parameter extraction of photovoltaic models from measured IV characteristics curves using a hybrid trust-region reflective algorithm. *Appl. Energy* **2018**, *232*, 36–53. [[CrossRef](#)]
20. Batzelis, E. Non-iterative methods for the extraction of the single-diode model parameters of photovoltaic modules: A review and comparative assessment. *Energies* **2019**, *12*, 358. [[CrossRef](#)]

21. Stornelli, V.; Muttillio, M.; De Rubeis, T.; Nardi, I. A new simplified five-parameter estimation method for single-diode model of photovoltaic panels. *Energies* **2019**, *12*, 4271. [[CrossRef](#)]
22. Mehta, H.K.; Warke, H.; Kukadiya, K.; Panchal, A.K. Accurate expressions for single-diode-model solar cell parameterization. *IEEE J. Photovolt.* **2019**, *9*, 803–810. [[CrossRef](#)]
23. Mathew, L.E.; Panchal, A.K. A complete numerical investigation on implicit and explicit PV single-diode-models using I-and V-approaches. *IEEE J. Photovolt.* **2021**, *11*, 827–837. [[CrossRef](#)]
24. ALQahtani, A.H. A simplified and accurate photovoltaic module parameters extraction approach using matlab. In Proceedings of the 2012 IEEE International Symposium on Industrial Electronics, Hangzhou, China, 28–31 May 2012; pp. 1748–1753. [[CrossRef](#)]
25. Abe, C.F.; Dias, J.B.; Haeberle, F.; Notton, G.; Faggianelli, G.A. Simplified Approach to Adjust IEC-60891 Equation Coefficients from Experimental Measurements With Long-Term Validation. *IEEE J. Photovolt.* **2020**, *11*, 496–503. [[CrossRef](#)]
26. Brust, J.; Burdakov, O.; Erway, J.; Marcia, R. Algorithm 1030: SC-SR1: MATLAB Software for Limited-memory SR1 Trust-region Methods. *arXiv* **2021**, arXiv:2209.12057. [[CrossRef](#)]
27. Rossi, C.; Buccella, P.; Stefanucci, C.; Sallese, J.M. SPICE modeling of photoelectric effects in silicon with generalized devices. *IEEE J. Electron Devices Soc.* **2018**, *6*, 987–995. [[CrossRef](#)]
28. Shockley, W. The Theory of p-n Junctions in Semiconductors and p-n Junction Transistors. *Bell Syst. Tech. J.* **1949**, *28*, 435–489. [[CrossRef](#)]
29. Yaqoob, S.J.; Saleh, A.L.; Motahhir, S.; Agyekum, E.B.; Nayyar, A.; Qureshi, B. Comparative study with practical validation of photovoltaic monocrystalline module for single and double diode models. *Sci. Rep.* **2021**, *11*, 19153. [[CrossRef](#)] [[PubMed](#)]
30. AbdulMawjood, K.; Refaat, S.S.; Morsi, W.G. Detection and prediction of faults in photovoltaic arrays: A review. In Proceedings of the 2018 IEEE 12th International Conference on Compatibility, Power Electronics and Power Engineering (CPE-POWERENG 2018), Doha, Qatar, 10–12 April 2018; pp. 1–8. [[CrossRef](#)]
31. Abe, C.F.; Dias, J.B.; Haeberle, F.; Notton, G.; Faggianelli, G.A. Experimental application of methods to compute solar irradiance and cell temperature of photovoltaic modules. *Sensors* **2020**, *20*, 2490. [[CrossRef](#)]
32. Bo, Q.; Cheng, W.; Khishe, M.; Mohammadi, M.; Mohammed, A.H. Solar photovoltaic model parameter identification using robust niching chimp optimization. *Sol. Energy* **2022**, *239*, 179–197. [[CrossRef](#)]
33. Gasparin, F.P.; Bühler, A.J.; Rampinelli, G.A.; Krenzinger, A. Statistical analysis of I–V curve parameters from photovoltaic modules. *Sol. Energy* **2016**, *131*, 30–38. [[CrossRef](#)]
34. Rawat, N.; Thakur, P.; Singh, A.K. A novel hybrid parameter estimation technique of solar PV. *Int. J. Energy Res.* **2022**, *46*, 4919–4934. [[CrossRef](#)]
35. da Luz, C.M.A.; Tofoli, F.L.; dos Santos Vicente, P.; Vicente, E.M. Assessment of the ideality factor on the performance of photovoltaic modules. *Energy Convers. Manag.* **2018**, *167*, 63–69. [[CrossRef](#)]
36. Belkaid, A.; Colak, I.; Kayisli, K.; Sara, M.; Bayindir, R. Modeling and simulation of polycrystalline silicon photovoltaic cells. In Proceedings of the 2019 7th International Conference on Smart Grid (icSmartGrid), Newcastle, NSW, Australia, 9–11 December 2019; pp. 155–158. [[CrossRef](#)]
37. Piliougine, M.; Guejia-Burbano, R.A.; Petrone, G.; Sánchez-Pacheco, F.J.; Mora-López, L.; Sidrach-de-Cardona, M. Parameters extraction of single diode model for degraded photovoltaic modules. *Renew. Energy* **2021**, *164*, 674–686. [[CrossRef](#)]
38. Ciulla, G.; Brano, V.L.; Di Dio, V.; Cipriani, G. A comparison of different one-diode models for the representation of I–V characteristic of a PV cell. *Renew. Sust. Energ. Rev.* **2014**, *32*, 684–696. [[CrossRef](#)]
39. Villalva, M.G.; Gazoli, J.R.; Ruppert Filho, E. Comprehensive approach to modeling and simulation of photovoltaic arrays. *IEEE Trans. Power Electron.* **2009**, *24*, 1198–1208. [[CrossRef](#)]

Disclaimer/Publisher’s Note: The statements, opinions and data contained in all publications are solely those of the individual author(s) and contributor(s) and not of MDPI and/or the editor(s). MDPI and/or the editor(s) disclaim responsibility for any injury to people or property resulting from any ideas, methods, instructions or products referred to in the content.